ECCOMAS Congress 2016
VII European Congress on Computational Methods in Applied Sciences and Engineering
M. Papadrakakis, V. Papadopoulos, G. Stefanou, V. Plevris (eds.)
Crete Island, Greece, 5–10 June 2016

THE UPLIFT CAPACITY OF HORIZONTAL PLATE ANCHORS IN SPATIALLY VARIABLE CLAY USING SPARSE POLYNOMIAL CHAOS EXPANSIONS

Tom Charlton[1] **and Mohamed Rouainia**[2]

[1] School of Civil Engineering and Geosciences, Newcastle University
Newcastle upon Tyne, NE1 7RU
e-mail: t.s.charlton@newcastle.ac.uk

[2] School of Civil Engineering and Geosciences, Newcastle University
Newcastle upon Tyne, NE1 7RU
e-mail: mohamed.rouainia@newcastle.ac.uk

Keywords: Offshore Geotechnics, Random Field, Finite Element Analysis, Polynomial Chaos.

Abstract. *As the offshore energy industry moves towards deepwater installations, plate anchors are increasingly used to moor floating production facilities. The ultimate holding capacity of a plate anchor in undrained clay has been widely investigated in scenarios where the undrained shear strength is a deterministic parameter, uniform or linearly increasing across the soil mass. However, it has been shown that bearing capacity of footings can be overestimated if spatial variability is not taken into account. In this paper, a least angle regression-based sparse polynomial chaos expansion is used to efficiently study the uplift capacity of horizontal plate anchors in spatially variable clay represented by a high-dimensional random field. The coefficients of the expansion are obtained from a set of finite element analyses and a range of anchor embedment ratios are modelled to investigate both shallow and deep anchor behaviour. The limiting cases of an attached and vented anchor, where the anchor is either fixed to or separable from the soil, are also considered. It is found that the probability of failure of vented anchors reduces with embedment depth due to a decrease in the variability of anchor capacity as shear planes lengthen. In the attached case, the probability of failure is dependent upon whether the anchor fails by a shallow or deep mechanism.*

1 INTRODUCTION

The recent move towards deepwater energy production has led to an increased interest in the analysis and design of anchoring systems. Plate anchors are commonly deployed to moor floating production facilities [1]. The holding capacity of plate anchors in undrained clay has been widely investigated, using both physical modelling and numerical analysis [2-4]. In these studies, the undrained shear strength is uniform or linearly increasing according to a defined trend. In reality, natural clay is a highly variable material and the values of engineering parameters fluctuate across the soil mass [5]. Spatial variability, generally represented by random fields, has been shown to influence mechanical behaviour in a range of geotechnical scenarios [6]. In footing problems, bearing capacity can be overestimated if spatial variability is not taken into account. This has recently been demonstrated by Li *et al.* [7] for the case of buried footings, representative of applications such as spudcan foundations for offshore drilling platforms. The effect on uplift capacity is less well-studied but clearly has important design implications.

In this paper, a least angle regression (LAR)-based sparse PCE [8] is used to efficiently study the uplift capacity of horizontal plate anchors in spatially variable undrained clay represented by a random field. LAR enables automatic selection of only the most influential terms of the expansion, reducing the number of model evaluations required to ensure a well-posed least squares regression problem and a good approximation. A finite element model is used to obtain the uplift capacity across a range of embedment ratios and the limiting cases of an ‘attached’ and ‘vented’ anchor, where the anchor is either fixed to or separable from the soil, are considered. The use of the PCE enables an accurate assessment of the probability of failure in comparison with current offshore design practice, where the mean undrained shear strength value is applied in combination with a partial safety factor.

2 SPARSE POLYNOMIAL CHAOS EXPANSIONS

Polynomial chaos expansions are a method for quantifying uncertainty in complex numerical models with input parameters represented by random variables. The model output can be approximated by expanding the response quantity onto a basis of orthogonal multivariate polynomials. If the model is denoted Γ, and is a function of M independent input random variables $\boldsymbol{\xi} = \{\xi_1, \dots, \xi_M\}^T$, this can be written as follows:

$$\Gamma(\boldsymbol{\xi}) = \sum_{\boldsymbol{\alpha} \in \mathbb{N}^M} a_{\boldsymbol{\alpha}} \psi_{\boldsymbol{\alpha}}(\boldsymbol{\xi}) \tag{1}$$

where $\psi_{\boldsymbol{\alpha}}$ is a multivariate polynomial basis and $a_{\boldsymbol{\alpha}}$ are deterministic coefficients which must be computed, for example by regression from a set of model evaluations. The sequence of non-negative integers $\boldsymbol{\alpha} = \{\alpha_1, \dots, \alpha_M\}$ is a multi-index representing the polynomial order associated with each random variable. The series is known as a polynomial chaos expansion and provides an analytical expression for the model response. For optimal convergence, the multivariate polynomial basis is chosen to be orthogonal with respect to the joint probability density function (PDF) of the input random variables. The multivariate, M-dimensional basis is constructed as a product of one-dimensional polynomials. In this paper, Gaussian input random variables are used with the corresponding Hermite polynomials.

The truncation, for computational purposes, of the infinite series in Eq. (1) was originally undertaken by keeping only those polynomials with degree less than or equal to the current PCE order p, i.e. $\sum_{i=1}^{M} \alpha_i \leq p$. The size of this basis is $P = \binom{M+p}{p}$ and the number of retained coefficients, and so the computational cost, grows dramatically as either the number of random variables M or polynomial order p is increased.

In a *sparse* polynomial chaos expansion (SPCE), only significant terms are retained in the polynomial basis, thus reducing the number of coefficients that must be computed. Firstly, the candidate set of terms can be reduced prior to analysis to remove high-order interactions likely to be insignificant. Blatman and Sudret [8] proposed a 'hyperbolic' PCE in which a q-norm of the multi-indices should be smaller than the current order as follows:

$$\|\boldsymbol{\alpha}\|_q = \left(\sum_{i=1}^{M} (\alpha_i)^q\right)^{1/q} \leq p \tag{2}$$

where $0 < q \leq 1$. This is a stricter requirement than the classical truncation scheme, which is recovered by setting $q = 1$.

The PCE is finally obtained as:

$$\Gamma(\boldsymbol{\xi}) \cong \hat{\Gamma}_p(\boldsymbol{\xi}) = \sum_{\|\boldsymbol{\alpha}\|_q \leq p} \hat{a}_{\boldsymbol{\alpha}} \psi_{\boldsymbol{\alpha}}(\boldsymbol{\xi}) \tag{3}$$

However, even after the size of the truncation set has been reduced, not all remaining terms will be significant. An efficient solution is to use least angle regression (LAR) [9] to select the basis functions that have most effect on the model response. In LAR, the predictors are progressively activated based on their correlation with the set of model outputs until either all predictors are active or, if the number of model evaluations $n \leq P$, $n - 1$ predictors are active.

The LAR-SPCE method [8] does not actually use the coefficients computed by LAR but instead uses the predictors retained in each step along the LAR path in a least squares regression. Hence a series of SPCEs are produced and their approximation performance is assessed by a corrected leave-one-out cross-validation error, denoted Q^{2*}, in order to select the best expansion for subsequent use. Details of the error estimate Q^{2*} can be found in [8]. To minimise the number of deterministic model evaluations an adaptive method is implemented in this study, with $q = 0.7$ and a maximum expansion order of 4.

3 PLATE ANCHOR UPLIFT CAPACITY

3.1 Description

Figure 1 shows the layout and notation of the plate anchor scenario analysed in this study. The dimensionless ratio H/B is used to describe the embedment depth at which the plate anchor is installed. Loads are applied perpendicular to the longitudinal axis of the anchor, with the ultimate pullout capacity denoted $Q_u (= q_u B)$. The pullout capacity in an undrained clay is generally expressed in terms of a dimensionless factor:

$$N_c = \frac{Q_u}{A s_u} \tag{4}$$

where A is the area of the plate and s_u is the undrained shear strength. In the deterministic analysis the clay is weightless and uniform, with s_u constant across the soil mass. If the anchor is embedded to such a depth that the failure mechanism becomes localised, the anchor can be described as 'deep'. In contrast, the failure mechanism of a shallow anchor will extend to ground level as the anchor is pulled out of the soil. It should be noted that this distinction is only relevant if soil and anchor are attached. Vented anchors only reach the ultimate capacity once the failure mechanism reaches the surface.

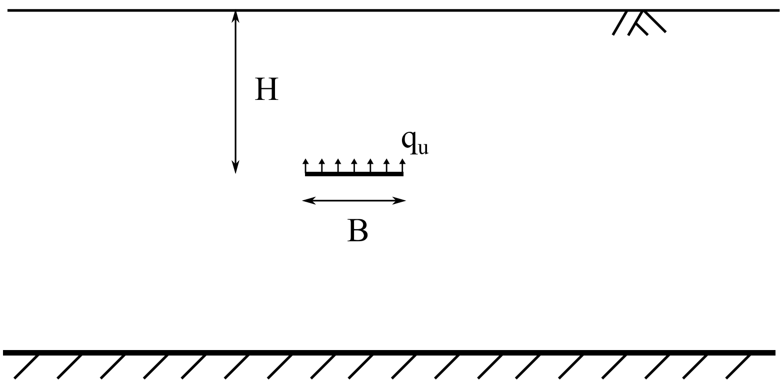

Figure 1. Layout and notation.

3.2 Representation of spatial variability

The spatial variability of undrained shear strength, s_u, is modelled as a lognormal random field. The mean (μ) of s_u is 10kPa and the coefficient of variation (COV) is taken to be 0.2, representing a typical variability based on results reported by Lacasse and Nadim [5]. In addition a constant rigidity index of E/s_u = 500 is assumed, where E is the elastic modulus. In statistical terms, E is therefore perfectly correlated with s_u and is generated from the same set of random variables.

An anisotropic square exponential autocorrelation function is adopted for s_u, with correlation distance 10m and 1m in the horizontal and vertical directions respectively. The lognormal random field can be generated as follows:

$$s_u(x,y) = \exp\left(\mu_{\mathrm{L,r}} + \sigma_{L,r} G(x,y)\right) \tag{5}$$

where μ_{L,s_u} is the mean of $ln(s_u)$, σ_{L,s_u} is the standard deviation of $ln(s_u)$, and $G(x,y)$ is a correlated Gaussian random field of zero mean and unit variance. The expansion optimal linear estimation (EOLE) method [10] is used to discretise the random field $G(x,y)$ on a rectangular grid, henceforth referred to as the stochastic mesh to indicate its independence from the deterministic model. The expansion is truncated to include M random variables, chosen such that at least 90% of the variance of $G(x,y)$ is captured.

3.3 Finite element model

The geotechnical FE software Plaxis 2D [11] is used as the deterministic model. The plate anchor, of width B = 2m, is modelled in plane strain and a range of embedment ratios are considered (H/B = 1, 2, 3, 6, and 10) in order to analyse both shallow and deep anchor behaviour.

Figure 2 shows a typical mesh, consisting of 15-node triangular elements, for an anchor embedded at H/B = 6. The anchor is modelled by a stiff plate element and the analysis is displacement-controlled. The clay is undrained and behaves according to the Mohr Coulomb model with friction angle φ = 0° and cohesion c = s_u. In the vented condition, an interface element is applied along the underside of the anchor with extensions at either end of 0.25B to avoid stress concentrations at the anchor tips. The section of interface adjacent to the anchor has no tensile strength so that separation of clay and plate occurs immediately when the anchor is displaced in the pullout direction. An interpolation procedure is used to transfer information from the stochastic mesh to the FE mesh. The deterministic capacity factors ($N_{c,det}$), using the mean value of s_u in a uniform soil profile, showed an overestimation of less than 2% compared with those reported by Yu *et al*. [4].

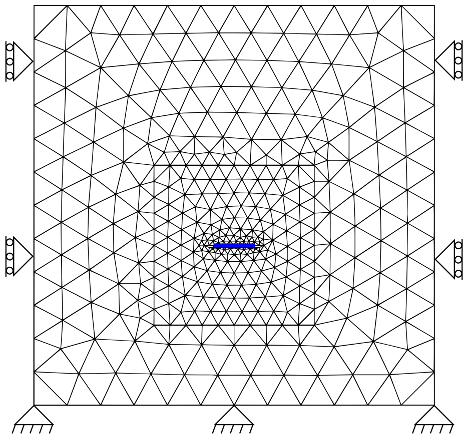

Figure 2. Typical FE mesh (H/B = 2).

4 RESULTS AND DISCUSSION

4.1 Performance of the LAR-SPCE method

Figure 3 shows the SPCE prediction of anchor capacity at H/B = 6 for the regression (or 'training') set and a test set of an additional 100 FE simulations not used in the regression. In this case, the random field is discretised using 50 standard Gaussian variables. To achieve the target accuracy, 1100 FE model evaluations were necessary in the attached condition, with 400 needed for a vented anchor. In both cases, a 3rd order expansion was found to be optimal, meaning the terms in the retained expansion have a maximum order of 3.

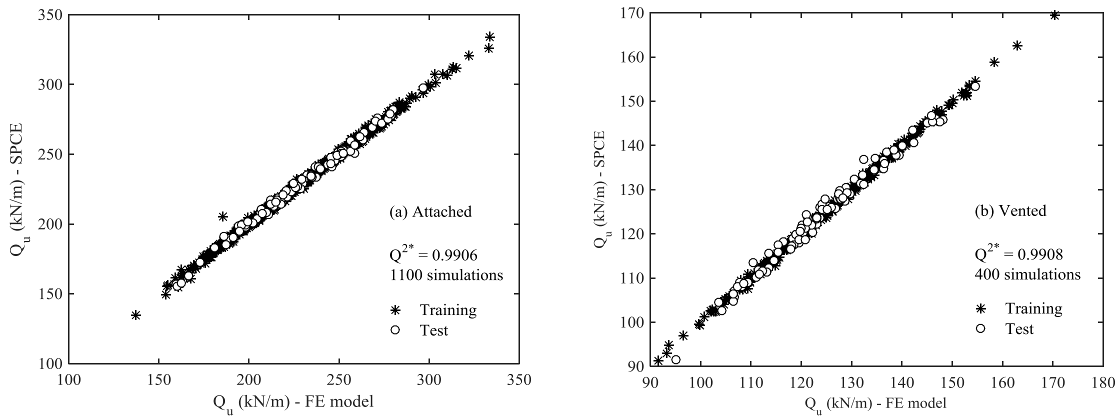

Figure 3. Retained SPCE approximation of FE model for a horizontal anchor with H/B = 6: training and test data for (a) attached and (b) vented anchor.

The strong linear relationship between the output of the FE and SPCE models demonstrates that the SPCE is able to produce an accurate approximation of the pullout capacity. This ensures that valid conclusions can be drawn about the probability distribution of the plate anchor capacity using an SPCE in place of the expensive FE model. The target accuracy of $Q^{2^*} = 0.99$ also provides acceptable performance for the number of simulations required; the rate of convergence tends to slow as the error reduces.

The number of FE model evaluations required to construct an SPCE of target accuracy is given in Table 1. In general, the computational effort is related to the number of variables necessary to discretise the field. However, in certain cases the nature of the failure mechanism can slow convergence. For example, the target value of Q^{2*} was not achieved for the attached anchor at H/B = 2. A very slow convergence was observed and the number of simulations was limited to 5000 for practical reasons. This slow convergence rate is a result of the anchor failing in a variety of different modes due to the spatial variability of the clay.

H/B	Random variables	Interface	Q^{2*}	FE simulations	Max. order
1	50	Attached	0.9915	800	3
		Vented	0.9908	400	3
2	60	Attached	0.9863	5000*	4
		Vented	0.9921	300	3
3	60	Attached	0.9908	1200	3
		Vented	0.9910	300	3
6	50	Attached	0.9906	1100	3
		Vented	0.9908	400	3
10	120	Attached	0.9910	3300	3
		Vented	0.9903	800	3

Table 1. Details of the retained SPCEs (*indicates target Q^{2*} was not reached).

In uniform (i.e. not spatially variable) clay, a deep mechanism forms with the shear plane localised around the anchor. In contrast, as shown in Figure 4, if the clay is spatially variable the failure mechanism can either be deep, being fully localised around the anchor, or shallow, involving a reverse end bearing mechanism, depending on the particular realisation of the random field. For this case the function $\Gamma(\xi)$ is not smooth, resulting in slow convergence of the SPCE. Note that 4th order terms were retained whereas in all other expansions only 3rd order polynomials were necessary. It is also clear that the critical embedment ratio, when the anchor transitions from a shallow to deep mechanism, is difficult to define exactly in spatially variable soil.

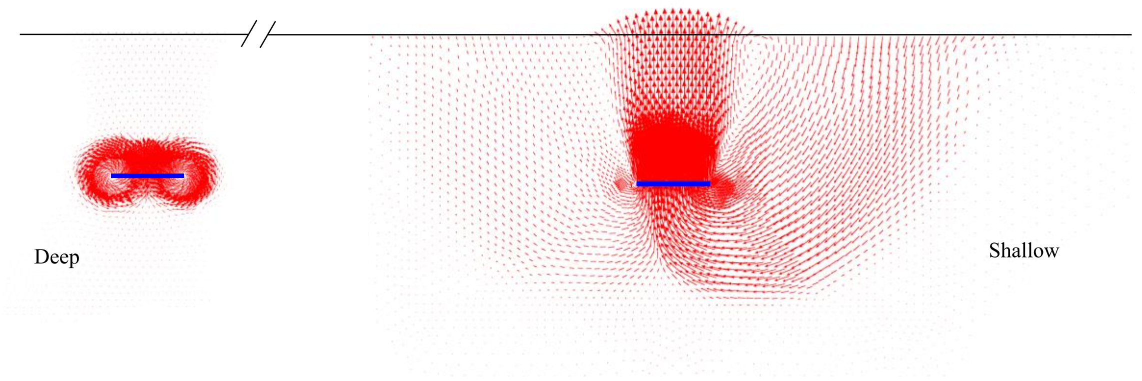

Figure 4. Failure mechanisms for an anchor embedded at H/B = 2 for two different random field realisations.

4.2 Statistics of the uplift capacity

The mean and standard deviation of the anchor capacity are obtained analytically from each SPCE. Figure 5 shows the mean, $\hat{\mu}_{Nc}$, and standard deviation, $\hat{\sigma}_{Nc}$, of the capacity factor in spatially variable clay across a range of embedment ratios. For comparison, the figure also shows the deterministic capacity factors. In both interface conditions, it can be seen that the mean capacity factor has a similar relationship with the embedment ratio as in the deterministic case and tends to be marginally (no more than 5%) lower than the equivalent deterministic capacity factor.

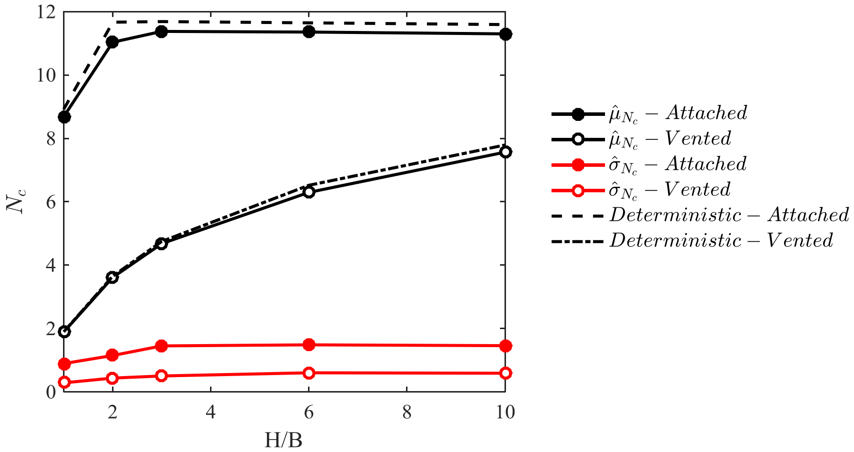

Figure 5. Mean, standard deviation, and deterministic capacity factors, N_c.

The variability of the pullout capacity for the different anchor configurations can be compared by considering the COV, as presented in Figure 6. For the vented case, the COV reduces with increasing embedment ratio. Li *et al*. [7] show that, for buried footings, a longer shear plane lowers the COV of the bearing capacity due to a greater spatial averaging effect. The same conclusion can be drawn from the failure mechanisms of the vented anchors. When anchor and soil are separable, the ultimate load is reached once the shear plane reaches the ground surface, regardless of anchor orientation. As H/B increases, the length of the shear plane is necessarily longer and the COV reduces. When the anchor and soil are attached, there is a distinct difference between the COV of ‘shallow’ and ‘deep’ anchors. If H/B is ≥ 3, the embedment ratio no longer affects the failure mechanism and COV is relatively constant.

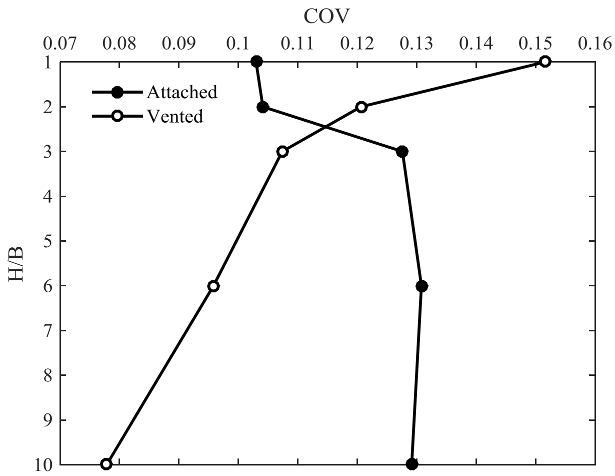

Figure 6. Coefficient of Variation (COV) against embedment ratio, H/B.

4.3 Probability of failure

The probability of failure can be defined as:

$$P_f = P\left(N_c < \frac{N_{c,det}}{FS}\right) \tag{6}$$

where FS is a factor of safety. This represents the probability that the capacity factor in spatially variable clay will be less than that predicted in a conventional numerical analysis with deterministic soil parameters.

Monte Carlo realisations of the SPCE are used to compute the probability of failure. To ensure a COV ≤ 0.1 for a probability of failure of 10^{-5}, which tends to be the lowest value of P_f considered in practice, the number of samples (n_{SPCE}) is 10^7. The estimated probability of failure is then:

$$\hat{P}_f = \frac{1}{n_{SPCE}} \sum_{i=1}^{n_{SPCE}} I\left(N_c^{(i)} < \frac{N_{c,det}}{FS}\right) \tag{7}$$

where I is the indicator function.

Figure 7 shows the probability of failure across a range of embedment depths as the factor of safety is increased from 1 to 3. If no factor of safety is used (FS = 1), the probability of failure ranges from 0.53 to 0.71 and is relatively independent of the interface condition. When a factor of safety is applied to $N_{c,det}$, the probability of failure can change greatly depending on the anchor configuration. If the anchor is vented, the probability of failure reduces as the anchor is embedded deeper into the clay. This is a direct result of the decreasing COV with depth observed for vented anchors. For the attached case, a distinction is again observed between deep and shallow anchors. As H/B increases, a constant probability of failure is reached as the failure mechanism is localised around the anchor.

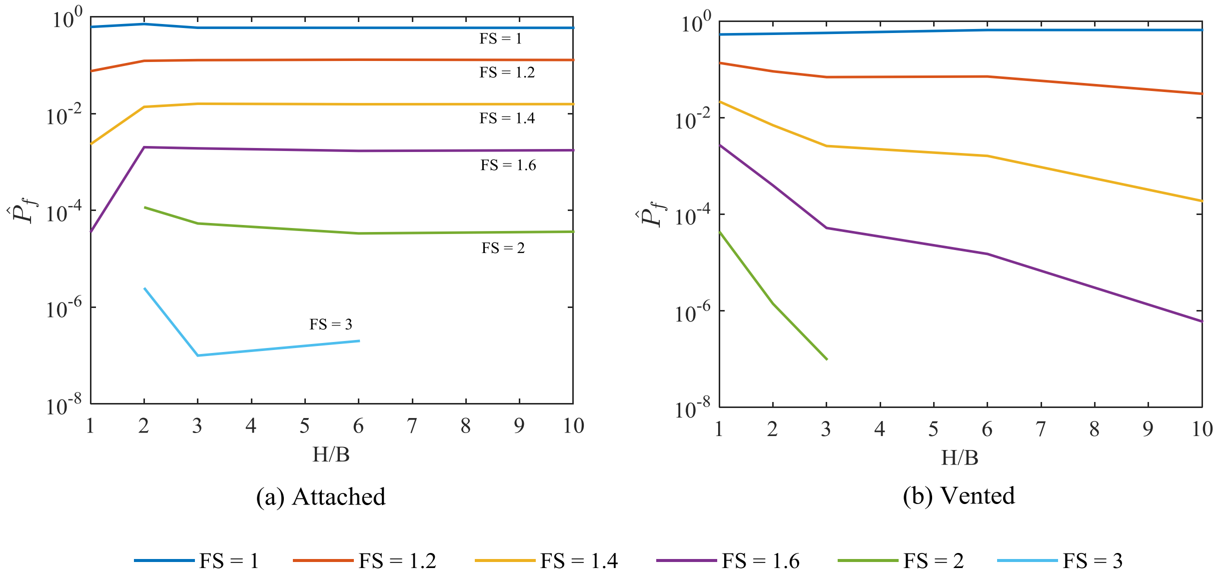

Figure 7. Probability of failure for (a) attached and (b) vented anchors when different factors of safety (FS) are applied to the deterministic capacity factor $(N_{c,det})$.

The recommended practice for the design of plate anchors DNV-RP-E302 [12] suggests a partial safety factor of 1.4 to account for uncertainty in "*$s_u(z)$ as it affects $R_s(z)$*" (where z indicates depth and R_s is the static resistance), as well as epistemic uncertainties resulting from, for example, the analytical model. The N_c values recommended by the design code correspond to attached anchors, and the mean of s_u is used as the characteristic value. The analysis presented here suggests that this factor may not be sufficient to account for natural spatial variability if the intended probability of failure is less than 10^{-2}. However, further investigation into the effect of COV and the autocorrelation structure of s_u is needed before concluding that the current design method is not conservative.

5 CONCLUSIONS

A study of the uplift capacity of a horizontal plate anchor in spatially variable clay has been conducted. An LAR-SPCE method was used to efficiently obtain the statistical moments of the anchor capacity and the probability of failure with respect to a conventional numerical analysis employing deterministic soil parameters. The probability of failure of vented anchors reduces with embedment depth due to a decrease in the variability of anchor capacity as shear planes lengthen. In the attached case, the probability of failure becomes relatively constant once the embedment ratio is large enough to ensure that the failure mechanism is localised around the anchor. The results of this study suggest that the partial factor used in current design practice may be not be sufficient to account for the spatial variability of undrained shear strength. Further research is necessary in order to better understand the effect of spatial variability on the ultimate capacity of plate anchors.

REFERENCES

[1] M.F. Randolph and S. Gourvenec, *Offshore geotechnical engineering*. Spon Press, 2011.

[2] R.K. Rowe and E.H. Davis, The behaviour of anchor plates in clay. *Géotechnique*, **32**(1), 9-23, 1982.

[3] R.S. Merifield, S.W. Sloan, and H.S. Yu, Stability of plate anchors in undrained clay. *Géotechnique*, **51**(2), 141-153, 2001.

[4] L. Yu, et al., Numerical study on plate anchor stability in clay. *Géotechnique*, **61**(3), 235-246, 2011.

[5] S. Lacasse and F. Nadim, *Uncertainties in Characterising Soil Properties*, in *Uncertainty in the Geologic Environment: from Theory to Practice*, C.D. Shackelford, P.P. Nelson, and M.J.S. Roth, Editors, New York: ASCE. 49-75. 1996.

[6] G.A. Fenton and D.V. Griffiths, *Risk Assessment in Geotechnical Engineering*. John Wiley & Sons, 2008.

[7] J. Li, Y. Tian, and M. Cassidy, Failure Mechanism and Bearing Capacity of Footings Buried at Various Depths in Spatially Random Soil. *Journal of Geotechnical and Geoenvironmental Engineering*, **141**(2), 2015.

[8] G. Blatman and B. Sudret, Adaptive sparse polynomial chaos expansion based on least angle regression. *Journal of Computational Physics*, **230**(6), 2345-2367, 2011.

[9] B. Efron, et al., Least angle regression. *Annals of Statistics*, **32**(2), 407-499, 2004.

[10] C. Li and A. Der Kiureghian, Optimal Discretization of Random Fields. *Journal of Engineering Mechanics*, **119**(6), 1136-1154, 1993.

[11] Plaxis, PLAXIS 2D 2012 - Reference Manual: Delft. 2012.

[12] DNV, *Design and Installation of Plate Anchors in Clay*, Det Norske Veritas (DNV): Norway. 2002.